Smooth electron waveguides in graphene

R. R. Hartmann, N. J. Robinson, and M. E. Portnoi*
School of Physics, University of Exeter, Stocker Road, Exeter EX4 4QL, United Kingdom
(Received 28 May 2010; published 23 June 2010)

We present exact analytical solutions for the zero-energy modes of two-dimensional massless Dirac fermions fully confined within a smooth one-dimensional potential $V(x)=-\alpha/\cosh(\beta x)$, which provides a good fit for potential profiles of existing top-gated graphene structures. We show that there is a threshold value of the characteristic potential strength α/β for which the first mode appears, in striking contrast to the nonrelativistic case. A simple relationship between the characteristic strength and the number of modes within the potential is found. An experimental setup is proposed for the observation of these modes. The proposed geometry could be utilized in future graphene-based devices with high on/off current ratios.

DOI: 10.1103/PhysRevB.81.245431 PACS number(s): 73.21.−b, 03.65.Ge, 03.65.Pm

I. INTRODUCTION

Klein proposed that relativistic particles do not experience exponential damping within a barrier like their nonrelativistic counterparts, and that as the barrier height tends toward infinity, the transmission coefficient approaches unity.[1] This inherent property of relativistic particles makes confinement nontrivial. Carriers within graphene behave as two-dimensional (2D) massless Dirac fermions, exhibiting relativistic behavior at sublight speed[2,3] owing to their linear dispersion, which leads to many optical analogies.[4–8] Klein tunneling through p-n junction structures in graphene has been studied both theoretically[5,9–17] and experimentally.[18–24] Quasibound states were considered in order to study resonant tunneling through various sharply terminated barriers.[5,11–13,17] We propose to change the geometry of the problem in order to study the propagation of fully confined modes along a smooth electrostatic potential much like photons moving along an optical fiber.

So far quasi-one-dimensional channels have been achieved within graphene nanoribbons,[3,25–28] however, controlling their transport properties requires precise tailoring of edge termination,[26] currently unachievable. In this paper we claim that truly bound modes can be created within bulk graphene by top-gated structures,[20–24] such as the one shown in Fig. 1(a). In an ideal graphene sheet at half-filling, the Fermi level is at the Dirac point and the density of states for a linear 2D dispersion vanishes. In realistic graphene devices the Fermi level can be set using the back gate. This is key to the realization of truly bound modes within a graphene waveguide, as zero-energy modes cannot escape into the bulk as there are no states to tunnel into. Moreover the electrostatic confinement isolates carriers from the sample edges, which are considered as a major source of intervalley scattering in clean graphene.[29]

In this paper we obtain an exact analytical solution for bound modes within a smooth electrostatic potential in pristine graphene at half-filling, count the number of modes and calculate the conductance of the channel. The conductance carried by each of these modes is comparable to the minimal conductivity of a realistic disordered graphene system.[2,30–32] For the considered model potential we show that there is a threshold potential characteristic strength (the product of the potential strength with its width), for which bound modes appear. Whereas a symmetric quantum well always contains a bound mode for nonrelativistic particles, we show that it is not the case for charge carriers in graphene.

II. FULLY CONFINED MODES IN A MODEL POTENTIAL

The Hamiltonian of graphene for a two-component Dirac wave function in the presence of a one-dimensional potential $U(x)$ is

$$\hat{H} = v_F(\sigma_x \hat{p}_x + \sigma_y \hat{p}_y) + U(x), \tag{1}$$

where $\sigma_{x,y}$ are the Pauli spin matrices, $\hat{p}_x=-i\hbar\frac{\partial}{\partial x}$ and $\hat{p}_y=-i\hbar\frac{\partial}{\partial y}$ are the momentum operators in the x and y directions, respectively, and $v_F \approx 1\times 10^6$ m/s is the Fermi velocity in graphene. In what follows we will consider smooth confining potentials, which do not mix the two nonequivalent valleys. All our results herein can be easily reproduced for the other valley. When Eq. (1) is applied to a two-component Dirac wave function of the form

$$e^{iq_y y}\begin{pmatrix}\Psi_A(x)\\ \Psi_B(x)\end{pmatrix},$$

where $\Psi_A(x)$ and $\Psi_B(x)$ are the wave functions associated with the A and B sublattices of graphene, respectively, and the free motion in the y direction is characterized by the wave vector q_y measured with respect to the Dirac point, the

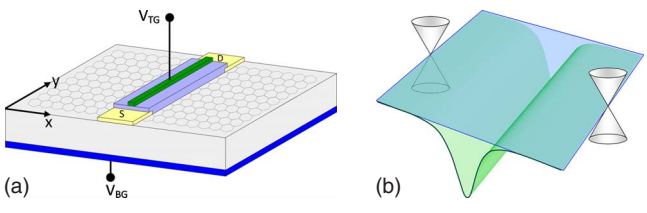

FIG. 1. (Color online) (a) A schematic of a Gedanken experiment for the observation of localized modes in graphene waveguides, created by the top gate (V_{TG}). The Fermi level is set using the back gate (V_{BG}) to be at the Dirac point ($\varepsilon_F=0$). (b) The electrostatic potential created by the applied top-gate voltage. The plane shows the Fermi-level position at $\varepsilon_F=0$.

following coupled first-order differential equations are obtained

$$[V(x)-\varepsilon]\Psi_A(x)-i\left(\frac{d}{dx}+q_y\right)\Psi_B(x)=0, \tag{2}$$

$$-i\left(\frac{d}{dx}-q_y\right)\Psi_A(x)+[V(x)-\varepsilon]\Psi_B(x)=0. \tag{3}$$

Here $V(x)=U(x)/\hbar v_F$ and energy ε is measured in units of $\hbar v_F$.

For the treatment of confined modes within a symmetric electron waveguide, $V(x)=V(-x)$, it is convenient to consider symmetric and antisymmetric modes. One can see from Eqs. (2) and (3) that $\Psi_A(x)$ and $\Psi_B(x)$ are neither even nor odd so we transform to symmetrized functions

$$\Psi_1=\Psi_A(x)-i\Psi_B(x), \quad \Psi_2=\Psi_A(x)+i\Psi_B(x).$$

The wave functions Ψ_1 and Ψ_2 satisfy the following system of coupled first-order differential equations:

$$[V(x)-(\varepsilon-q_y)]\Psi_1-\frac{d\Psi_2}{dx}=0, \tag{4}$$

$$\frac{d\Psi_1}{dx}+[V(x)-(\varepsilon+q_y)]\Psi_2=0. \tag{5}$$

It is clear from Eqs. (4) and (5) that Ψ_1 and Ψ_2 have opposite parity.

For an ideal graphene sheet at half-filling the conductivity is expected to vanish due to the vanishing density of states. When the Fermi energy is at the Dirac point ($\varepsilon=0$) there are no charge carriers within the system so graphene is a perfect insulator. However all available experiments demonstrate nonvanishing minimal conductivity[2,3,30] of the order of e^2/h which is thought to be due to disorder within the system[3,31–33] or finite-size effects.[34,35] In order to study confined states within and conductance along an electron waveguide it is necessary to use the back gate to fix the Fermi energy (ε_F) at zero, as shown in Fig. 1(b). Note that Fig. 1(a) is just a schematic of the proposed experimental geometry and that side contacts may be needed to maintain the "bulk" Fermi level at zero energy. The conductivity of the graphene sheet is a minimum and for a square sample the conductance is of the order of the conductance carried by a single mode within a waveguide. Thus the appearance of confined modes within the electron waveguide will drastically change the conductance of a graphene flake. Indeed each mode will contribute $4e^2/h$ taking into account valley and spin degeneracy. For device applications the sample should be designed in such a way that the contribution to the conductance from the confined modes is most prominent. In the ideal case, the conductivity of the channel would be the only contribution to that of the graphene sheet. When $\varepsilon_F\neq 0$, the conductivity will be dominated by the 2D Fermi sea of electrons throughout the graphene sheet. Henceforth, we shall consider the modes for $\varepsilon=0$.

We shall consider truly smooth potentials, allowing us to avoid the statement of "sharp but smooth" potentials, which is commonly used to neglect intervalley mixing for the tunneling problem.[9–13] Furthermore, we are interested in potentials that vanish at infinity and have at least two fitting parameters, characterizing their width and strength, in order to fit experimental potential profiles.[19–24] Let us consider the following class of potentials, which satisfy the aforementioned requirements:

$$V(x)=-\frac{\alpha}{\cosh^{\lambda}(\beta x)}, \tag{6}$$

where α, β, and λ are positive parameters. The negative sign in Eq. (6) reflects a potential well for electrons and similar results can easily be obtained for holes by changing the sign of $V(x)$. Notably $\lambda=2$ is the familiar case of the Pöschl-Teller potential, which has an analytic solution for the nonrelativistic case.[36] It is shown in the Appendix that the model potential Eq. (6) with $\lambda=1$ provides an excellent fit to a graphene top-gate structure.

Eliminating Ψ_2 (Ψ_1) reduces the system of Eqs. (4) and (5) to a single second-order differential equation for Ψ_1 (Ψ_2), which for the potential given by Eq. (6) and $\varepsilon=0$ becomes

$$\frac{d^2\Psi_{1,2}}{dz^2}+\lambda\tanh(z)\frac{\omega\cosh^{-\lambda}(z)}{\omega\cosh^{-\lambda}(z)\pm\Delta}\frac{d\Psi_{1,2}}{dz}+[\omega^2\cosh^{-2\lambda}(z)-\Delta^2]\Psi_{1,2}=0, \tag{7}$$

where we use the dimensionless variables $z=\beta x$, $\Delta=q_y/\beta$, and $\omega=\alpha/\beta$. For $\lambda=1$, the change of variable $\xi=\tanh(z)$ allows Eq. (7) to be reduced to a set of hypergeometric equations yielding the following non-normalized bound solutions for $\Delta>0$

$$\Psi_{1,2}=\pm(1+\xi)^p(1-\xi)^q\times{}_2F_1\left(p+q-\omega,p+q+\omega;2p+\frac{1}{2};\frac{1+\xi}{2}\right)+(-1)^n(1+\xi)^q(1-\xi)^p\times{}_2F_1\left(p+q-\omega,p+q+\omega;2p+\frac{1}{2};\frac{1-\xi}{2}\right), \tag{8}$$

where in order to terminate the hypergeometric series it is necessary to satisfy $p=\frac{1}{2}(\omega-n)+\frac{1}{4}$, $q=\frac{1}{2}(\omega-n)-\frac{1}{4}$, and $\Delta=\omega-n-\frac{1}{2}$, where n is a positive integer. Though we have assumed that ω is positive, one can see that the structure of the solutions in Eq. (8) remains unchanged with the change of sign of ω, reflecting electron-hole symmetry. In order to avoid a singularity at $\xi=\pm 1$ we require that both $p>0$ and $q>0$ and obtain the condition that $\omega-n>\frac{1}{2}$. It should be noted that this puts an upper limit on n, the order of termination of the hypergeometric series. Notably the first mode occurs at $n=0$, thus there is a lower threshold of $\omega>\frac{1}{2}$ for

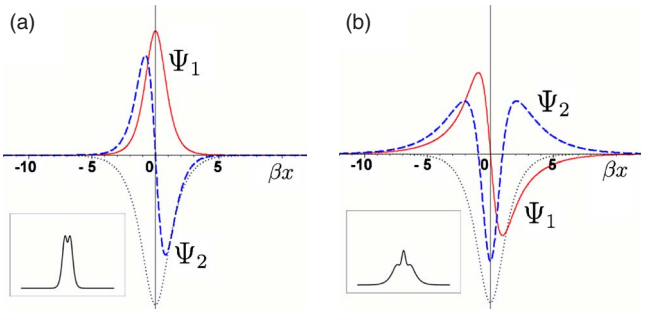

FIG. 2. (Color online) The wave functions Ψ_1 (solid line) and Ψ_2 (dashed line) are shown for $\omega=2$ for (a) the first ($n=0$) mode and (b) the second ($n=1$) mode. A potential profile is provided as a guide for the eye (dotted line). The insets show the electron-density profile for the corresponding modes.

which bound modes appear. Hence within graphene, quantum wells are very different to the nonrelativistic case; bound states are not present for any symmetric potential, they are only present for significantly strong or wide potentials such that $\omega=\alpha/\beta>\frac{1}{2}$.

Let us consider the first mode ($n=0$) in Eq. (8) which appears within the electronic waveguide with increasing ω. In this case the hypergeometric function is unity, and the normalized wave functions are

$$\Psi_{1,2}=A_{1,2}[(1+\xi)^{\omega/2-1/4}(1-\xi)^{\omega/2+1/4} \pm (1+\xi)^{\omega/2+1/4}(1-\xi)^{\omega/2-1/4}], \tag{9}$$

where $A_{1,2}$ is given by

$$A_{1,2}=\left\{\frac{\beta(2\omega-1)\Gamma(\omega)\Gamma\left(\omega+\frac{1}{2}\right)}{4\sqrt{\pi}\left[2\Gamma^2\left(\omega+\frac{1}{2}\right)\pm(2\omega-1)\Gamma^2(\omega)\right]}\right\}^{1/2}, \tag{10}$$

where $\Gamma(z)$ is the Gamma function. As expected, the two functions given by Eq. (9) are of different parity, thus unlike the nonrelativistic case there is an odd function corresponding to the first confined mode. This leads to a threshold in the characteristic potential strength ω at which the first confined mode appears; much like in the conventional quantum well, where the first odd state appears only for a sufficiently deep or wide potential well. In Fig. 2 we present Ψ_1, Ψ_2, and the corresponding electron-density profiles for the first and second-bound modes for the case of $\omega=2$. The shape of the confinement potential is shown for guidance within the same figure. The charge-density profile for these modes differs drastically from the nonrelativistic case. The first mode ($n=0$) has a dip in the middle of the potential well whereas the second mode ($n=1$) has a maximum. This is a consequence of the complex two-component structure of the wave functions.

For negative values of Δ, Ψ_1, and Ψ_2 switch parity such that $\Psi_{1,2}(-\Delta)=\Psi_{2,1}(\Delta)$. This means backscattering within a channel requires a change in parity of the wave functions in the x direction. Notably, when another nonequivalent Dirac valley is considered, one finds that there are modes of the same parity propagating in the opposite direction. However intervalley scattering requires a very short-range potential or proximity to the sample edges. Thus for smooth scattering potentials backscattering should be strongly suppressed. Such suppression should result in an increase in the mean-free path of the channel compared to that of graphene. This is similar to the suppression of backscattering in carbon nanotubes,[37] where the ballistic regime is believed to persist up to room temperature with a mean-free path exceeding one micrometer.[38,39] In some sense the considered waveguide can be thought of as a carbon nanotubelike structure with parameters controlled by the top gate.

Notably, our results are also applicable for the case of a one-dimensional massive particle which is confined in the same potential. This can be achieved by the substitution $|q_y|\rightarrow mv_F/\hbar$ into Eqs. (4) and (5), where the gap is given by $2mv_F^2$. Hence in the massless 2D case the momentum along the waveguide plays the same role as the gap in the massive one-dimensional case. Therefore, in a massive one-dimensional Dirac system (such as a narrow-gap carbon nanotube) there exists a bound state in the middle of the gap for certain values of the characteristic strength of the potential.

The number of modes N_ω at a fixed value of ω is the integer part of $\omega+\frac{1}{2}$ herein denoted $N_\omega=\lfloor\omega+\frac{1}{2}\rfloor$. The conductance of an ideal one-dimensional channel characterized by ω is found using the Landauer formula to be $G_\omega=4N_\omega e^2/h$. By modulating the parameters of the potential, one can increase the conductance of the channel from zero in jumps of $4e^2/h$. The appearance of the first and further confined modes within the conducting channel modifies both the strength and the profile of the potential. This nonlinear screening effect[14,15] is neglected in the above expression for G_ω and shall be a subject of future investigation.

Exact solutions for confined modes can also be found for the Pöschl-Teller potential, $V(x)=-\alpha/\cosh^2(\beta x)$, which corresponds to $\lambda=2$ in Eq. (7). Wave functions can be expressed via Heun polynomials in variable $\xi=\tanh(\beta x)$.

III. DISCUSSION AND CONCLUSIONS

All the results obtained in this paper have been for a specific potential. However, general conclusions can be drawn from these results for any symmetric potential. Namely, the product of the potential strength and its width dictates the number of confined modes within the channel.[40] Moreover, this product has a threshold value for which the first mode appears. The width of the potential is defined by the geometry of the top-gate structure and the strength of the potential is defined by the voltage applied to the top gate. The mean-free path of electrons within graphene is of the order of 100-nm and sub-100-nm width gates have been reported in the literature,[19–24] making quantum effects relevant. The number of modes within such top-gated structures is governed by the strength of the potential with new modes appearing with increasing potential strength. In a top-gate

structure modeled by our potential with a width at half-maximum of 50 nm, the first-bound mode should appear for a potential strength of approximately 17 meV and further modes should appear with increasing potential strength in steps of 34 meV, which corresponds to 395 K. Therefore a noticeable change in conductivity should be observed in realistic structures even at room temperature. This is similar to the quantum-Hall effect which is observed in graphene at room temperature.[41] A change in geometry, from normal transmission to propagation along a potential allows graphene to be used as a switching device.

In summary, we show that contrary to the widespread belief, truly confined (nonleaky) modes are possible in graphene in a smooth electrostatic potential vanishing at infinity. Full confinement is possible for zero-energy modes due to the vanishing density of states at the charge-neutrality point. We present exact analytical solutions for fully confined zero-energy modes in the potential $V(x)=-\alpha/\cosh(\beta x)$, which provides a good fit (see Appendix) to experimental potential profiles in existing top-gate structures.[19–24] Within such a potential there is a threshold value of $\omega=\alpha/\beta$ for which bound modes first appear, which is different to conventional nonrelativistic systems. We found a simple relation between the number of confined modes and the characteristic potential strength ω. The threshold potential strength enables on/off behavior within the graphene waveguide and suggests future device applications. The existence of bound modes within smooth potentials in graphene may provide an additional argument in favor of the mechanism for minimal conductivity, where charge puddles lead to a percolation network of conducting channels.[33]

There are experimental challenges which need to be resolved in order to observe confined modes in graphene waveguides. These include creating narrow gates and thin dielectric layers as well as optimizing the geometry of the sample to reduce the background conductance. Our work also poses further theoretical problems, including the study of nonlinear screening, many-body effects, parity changing backscattering, and intervalley scattering within the channel.

The study of quasi-one-dimensional channels within conventional semiconductor systems has lead to many interesting effects. Many problems are still outstanding, including the 0.7 anomaly in the ballistic conductance which is a subject of extensive experimental and theoretical study.[42] We envisage that the ability to produce quasi-one-dimensional channels within graphene will reveal new and nontrivial physics.

ACKNOWLEDGMENTS

We are grateful to A. V. Shytov, A. S. Mayorov, Y. Kopelevich, J. C. Inkson, D. C. Mattis, and N. Hasselmann for valuable discussions, and we thank ICCMP Brasília and UNICAMP for hospitality. This work was supported by EPSRC (R.R.H. and N.J.R.), EU projects ROBOCON (Grant No. FP7-230832) and TerACaN (Grant No. FP7-230778), MCT, IBEM, and FINEP (Brazil).

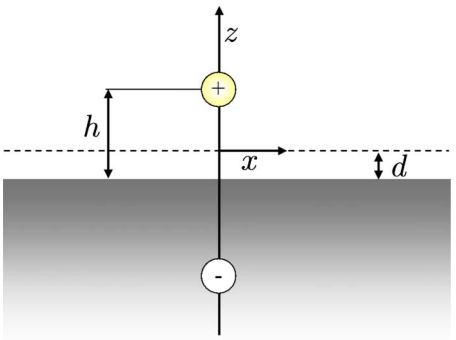

FIG. 3. (Color online) The simplified geometry used to obtain the model potential. The image charge is shown for convenience.

APPENDIX: POTENTIAL DUE TO A WIRE ABOVE A GRAPHENE SHEET

To illustrate the relevance of our model potential to realistic top-gate structures we provide a simple calculation of the potential distribution in the graphene plane for a simplified top-gate structure. Figure 3 shows the model that we use for our estimate. We consider a wire of radius r_0, separated by distance h from a metallic substrate (i.e., doped Si) and calculate the potential profile in the graphene plane separated from the same substrate by distance d. We are interested in the case when the Fermi level in graphene is at zero energy (the Dirac point) hence we assume the absence of free carriers in graphene. We also assume the absence of any dielectric layers but the problem can be generalized in such an instance.

One can easily show that the potential energy for an electron in the graphene plane is given by

$$U(x) = \frac{e\widetilde{\phi_0}}{2}\ln\left[\frac{x^2+(h-d)^2}{x^2+(h+d)^2}\right], \tag{A1}$$

where $\widetilde{\phi_0}=\phi_0/\ln[(2h-r_0)/r_0]$, ϕ_0 is the voltage applied between the top electrode and metallic substrate and e is the

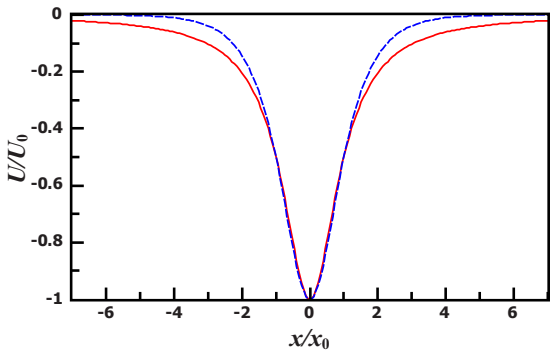

FIG. 4. (Color online) A comparison between the potential created by a wire suspended above the graphene plane (solid line) and the $-U_0/\cosh(\beta x)$ potential with the same half-width at half-maximum (dashed line).

absolute value of the electron charge. One can see that this potential behaves as

$$U(x) \approx -U_0 + e\widetilde{\phi}_0 \frac{2hd}{(h^2-d^2)^2}x^2, \quad x \ll (h-d),$$

$$U(x) \approx -e\widetilde{\phi}_0 \frac{2hd}{x^2}, \quad x \gg (h+d).$$

The depth of the potential well is given by

$$U_0 = e\phi_0 \left[\frac{\ln\left(\frac{h+d}{h-d}\right)}{\ln\left(\frac{2h-r_0}{r_0}\right)} \right]$$

and the half-width at half-maximum (HWHM) is given by $x_0=\sqrt{h^2-d^2}$. In Fig. 4 we show a comparison between the potential given by Eq. (A1) and the potential considered in our paper with the same HWHM and potential strength. Clearly the potential given by $-U_0/\cosh(\beta x)$, provides a significantly better approximation than that of the square-well potential.

*m.e.portnoi@exeter.ac.uk

[1] O. Klein, Z. Phys. **53**, 157 (1929).
[2] K. S. Novoselov, A. K. Geim, S. V. Morozov, D. Jiang, M. I. Katsnelson, I. V. Grigorieva, S. V. Dubonos, and A. A. Firsov, Nature (London) **438**, 197 (2005).
[3] A. H. Castro Neto, F. Guinea, N. M. R. Peres, K. S. Novoselov, and A. K. Geim, Rev. Mod. Phys. **81**, 109 (2009).
[4] V. V. Cheianov, V. I. Fal'ko, and B. L. Altshuler, Science **315**, 1252 (2007).
[5] A. V. Shytov, M. S. Rudner, and L. S. Levitov, Phys. Rev. Lett. **101**, 156804 (2008).
[6] L. Zhao and S. Yelin, arXiv:0804.2225 (unpublished); Phys. Rev. B **81**, 115441 (2010).
[7] C. W. J. Beenakker, R. A. Sepkhanov, A. R. Akhmerov, and J. Tworzydło, Phys. Rev. Lett. **102**, 146804 (2009).
[8] F. M. Zhang, Y. He, and X. Chen, Appl. Phys. Lett. **94**, 212105 (2009).
[9] M. I. Katsnelson, K. S. Novoselov, and A. K. Geim, Nat. Phys. **2**, 620 (2006).
[10] V. V. Cheianov and V. I. Fal'ko, Phys. Rev. B **74**, 041403(R) (2006).
[11] J. M. Pereira, Jr., V. Mlinar, F. M. Peeters, and P. Vasilopoulos, Phys. Rev. B **74**, 045424 (2006).
[12] T. Ya. Tudorovskiy and A. V. Chaplik, JETP Lett. **84**, 619 (2006).
[13] J. M. Pereira, Jr., P. Vasilopoulos, and F. M. Peeters, Appl. Phys. Lett. **90**, 132122 (2007).
[14] L. M. Zhang and M. M. Fogler, Phys. Rev. Lett. **100**, 116804 (2008).
[15] M. M. Fogler, D. S. Novikov, L. I. Glazman, and B. I. Shklovskii, Phys. Rev. B **77**, 075420 (2008).
[16] C. W. J. Beenakker, Rev. Mod. Phys. **80**, 1337 (2008).
[17] H. C. Nguyen, M. T. Hoang, and V. L. Nguyen, Phys. Rev. B **79**, 035411 (2009).
[18] J. R. Williams, L. DiCarlo, and C. M. Marcus, Science **317**, 638 (2007).
[19] B. Huard, J. A. Sulpizio, N. Stander, K. Todd, B. Yang, and D. Goldhaber-Gordon, Phys. Rev. Lett. **98**, 236803 (2007).
[20] B. Özyilmaz, P. Jarillo-Herrero, D. Efetov, D. A. Abanin, L. S. Levitov, and P. Kim, Phys. Rev. Lett. **99**, 166804 (2007).
[21] R. V. Gorbachev, A. S. Mayorov, A. K. Savchenko, D. W. Horsell, and F. Guinea, Nano Lett. **8**, 1995 (2008).
[22] G. Liu, J. Velasco, Jr., W. Bao, and C. N. Lau, Appl. Phys. Lett. **92**, 203103 (2008).
[23] N. Stander, B. Huard, and D. Goldhaber-Gordon, Phys. Rev. Lett. **102**, 026807 (2009).
[24] A. F. Young and P. Kim, Nat. Phys. **5**, 222 (2009).
[25] M. Y. Han, B. Özyilmaz, Y. Zhang, and P. Kim, Phys. Rev. Lett. **98**, 206805 (2007).
[26] L. Brey and H. A. Fertig, Phys. Rev. B **73**, 235411 (2006).
[27] P. G. Silvestrov and K. B. Efetov, Phys. Rev. Lett. **98**, 016802 (2007).
[28] N. M. R. Peres, J. N. B. Rodrigues, T. Stauber, and J. M. B. Lopes dos Santos, J. Phys.: Condens. Matter **21**, 344202 (2009).
[29] D. W. Horsell, A. K. Savchenko, F. V. Tikhonenko, K. Kechedzhi, I. V. Lerner, and V. I. Fal'ko, Solid State Commun. **149**, 1041 (2009).
[30] Y.-W. Tan, Y. Zhang, K. Bolotin, Y. Zhao, S. Adam, E. H. Hwang, S. Das Sarma, H. L. Stormer, and P. Kim, Phys. Rev. Lett. **99**, 246803 (2007).
[31] P. M. Ostrovsky, I. V. Gornyi, and A. D. Mirlin, Phys. Rev. Lett. **98**, 256801 (2007).
[32] S. Adam, E. H. Hwang, V. M. Galitski, and S. Das Sarma, Proc. Natl. Acad. Sci. U.S.A. **104**, 18392 (2007).
[33] V. V. Cheianov, V. I. Fal'ko, B. L. Altshuler, and I. L. Aleiner, Phys. Rev. Lett. **99**, 176801 (2007).
[34] M. I. Katsnelson, Eur. Phys. J. B **51**, 157 (2006).
[35] J. Tworzydło, B. Trauzettel, M. Titov, A. Rycerz, and C. W. J. Beenakker, Phys. Rev. Lett. **96**, 246802 (2006).
[36] G. Pöschl and E. Teller, Z. Phys. **83**, 143 (1933).
[37] T. Ando, T. Nakanishi, and R. Saito, J. Phys. Soc. Jpn. **67**, 2857 (1998).
[38] M. P. Anantram and F. Léonard, Rep. Prog. Phys. **69**, 507 (2006).
[39] O. V. Kibis, M. Rosenau da Costa, and M. E. Portnoi, Nano Lett. **7**, 3414 (2007), and references therein.
[40] For example, in a finite square well of width d and depth U_0, new zero-energy states appear when $U_0 d/\hbar v_F=(2n+1)\pi/2$, where $n=0,1,2,\ldots$.
[41] K. S. Novoselov, Z. Jiang, Y. Zhang, S. V. Morozov, H. L. Stormer, U. Zeitler, J. C. Maan, G. S. Boebinger, P. Kim, and A. K. Geim, Science **315**, 1379 (2007).
[42] I. A. Shelykh, M. Rosenau da Costa, and A. C. Seridonio, J. Phys.: Condens. Matter **20**, 164214 (2008), and references therein.